WELDING RESEARCH

SUPPLEMENT TO THE *WELDING JOURNAL*, FEBRUARY 1988

**Sponsored by the American Welding Society and the Welding Research Council**

All papers published in the *Welding Journal's* Welding Research Supplement undergo Peer Review before publication for: 1) originality of the contribution; 2) technical value to the welding community; 3) prior publication of the material being reviewed; 4) proper credit to others working in the same area; and 5) justification of the conclusions, based on the work performed.

The names of the more than 170 individuals serving on the AWS Peer Review Panel are published periodically. All are experts in specific technical areas, and all are volunteers in the program.

# Power and Current Distributions in Gas Tungsten Arcs

*An improved method of data analysis for determining power- and current-density distributions in welding arcs has been developed*

**BY M. LU AND S. KOU**

ABSTRACT. The power- and current-density distributions in a welding arc can significantly affect heat and fluid flow in the weld pool during arc welding, which in turn affects important weld characteristics such as weld penetration, segregation, gas porosity and solidification structure. In order to provide quantitative information for studying heat and fluid flow in the weld pool, an experimental study was carried out to measure the power- and current-density distributions in gas tungsten arcs using a split-anode technique. The method for determining the power- and current-density distributions from the experimental data generated by the split-anode technique is rather critical. A new, improved method developed in the present study, as well as four other previous methods, were employed to determine the power- and current-density distributions from the experimental data. The validity of the approximation of the Gaussian distribution was examined, and the effects of the arc length, arc current and electrode diameter were observed.

*M. LU and S. KOU are, respectively, Graduate Student and Professor at the Department of Metallurgical and Mineral Engineering, University of Wisconsin, Madison, Wis.*

## Introduction

In the classical welding heat flow theory of Rosenthal (Ref. 1), the heat source was treated as a point. In reality, however, the heat source is more often finite in size than merely a point. In gas tungsten arc welding, for instance, the arc covers a certain area on the workpiece surface, depending on the welding condition used. The welding experiments conducted by Savage, *et al.* (Ref. 2), and especially by Key, *et al.* (Ref. 3), have strongly suggested that the distributions of power and current in a gas tungsten arc can significantly affect the geometry of the resultant weld bead — a more constricted arc tends to produce a higher depth/width ratio of the weld bead. Kou, *et al.* (Ref. 4), have developed a heat-flow model and have demonstrated with the help of the model the effect of the power-density distribution on the geometry of gas tungsten arc welds. More recently, Oreper, *et al.* (Refs. 5-7), and Kou, *et al.* (Refs. 8-12), have developed fluid-flow models and have demonstrated with the help of the models the effect of the power- and current-density distributions on weld pool convection and penetration in gas tungsten arc welds. To effectively use these models to simulate heat and fluid flow during welding, the power- and current-density distributions of the welding arc must be specified first.

In order to better understand the pow-

**KEY WORDS**

Gas Tungsten Arcs
Power Density
Current Density
Density Distribution
Welding Arcs
Data Analysis
Heat and Fluid Flow
Split-Anode Technique
Non-Parametric Minimization
Minimization

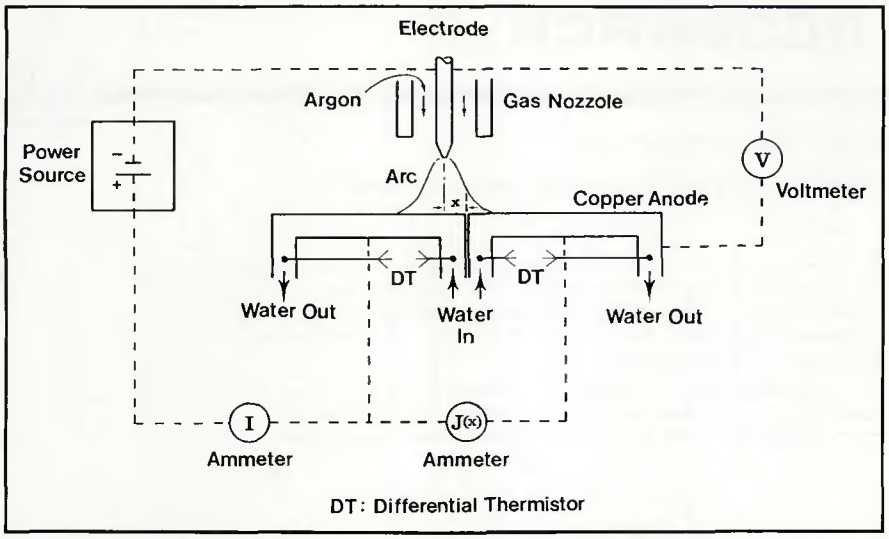


*Fig. 1—Schematic illustration of the split-anode technique*

er- and current-density distributions in welding arcs and, at the same time, provide quantitative information for studying heat and fluid flow during arc welding, it is essential to have a reliable method for determining such distributions. This, in fact, is the objective of the present study.

The power- and current-density distributions in electric arcs have been measured by Nestor (Refs. 13, 14) using a split-anode technique. Schoeck (Refs. 15, 16) has also measured the power-density distribution in electric arcs, using both a split-anode technique identical to that used by Nestor and a point-probe-anode technique. However, neither of the two investigators was concerned with welding arcs, and the experimental conditions used were quite different from those encountered in arc welding. Nevertheless, both studies have provided useful information about the basic experimental techniques and methods of data analysis for determining the power- and current-density distributions.

Recently, Tsai (Ref. 17) had adopted the same split-anode technique previously used by Nestor and Schoeck to measure the power- and current-density distributions in gas tungsten welding arcs. Three different methods of data analysis were used to determine the distribution curves from the split-anode data. Due to difficulties associated with each of the three methods, however, all three methods were used, and the results were compared to attain the best solutions for the power- and current-density distributions.

During the early stage of the present study, the three data analysis methods used by Tsai were also adopted, and rather abnormal distribution curves were frequently obtained. It was soon realized that the method of data analysis is very critical, and a reliable method must be found. Two additional methods were then employed, including the new method developed in the present study.

*Fig. 2—The split-anode coordinate system. The shaded area represents the heat flux to the right dee, i.e., F(x). R and x are the arc radius and position, respectively*

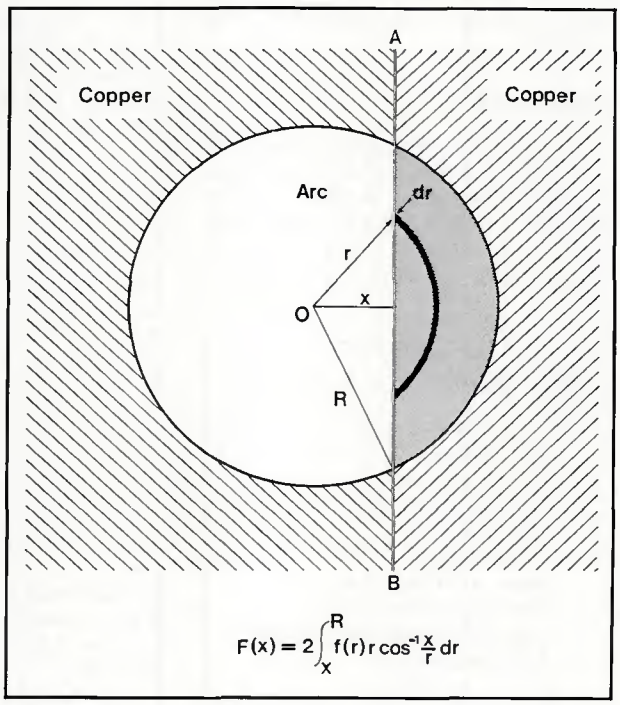


## Experimental Technique

The split-anode technique (Refs. 13, 15) was used in the present study for measuring the power- and current-density distributions in gas tungsten arcs. The basic principle of this technique is illustrated schematically in Figs. 1 and 2. As shown, the center of the arc (O) is a distance x to the left of the splitting plane AB in the copper anode. The heat transfer rate to the right anode section is described as follows.

$$F(x) = 2\int_x^R f(r)\, r \cos^{-1}(x/r)\, dr \qquad (1)$$

where R is the radius of the arc and f(r) is the heat transfer rate per unit area over the annular zone bounded by radii r and r + dr. The integrated function F(x) is measured directly, while the radial distribution f(r) is the function to be determined. From Equation 1, the slope of the function F(x) is as follows.

$$F'(x) = -2\int_x^R \frac{f(r)\, r}{\sqrt{r^2-x^2}}\, dr \qquad (2)$$

The above equation is an Abel integral equation, and the solution f(r) is as follows.

$$f(r) = \frac{1}{\pi}\int_x^R \frac{F''(x)}{\sqrt{x^2-r^2}}\, dx \qquad (3)$$

In the above equation, F″(x) is the second derivative of the heat transfer rate to the right anode section F(x) with respect to the arc position x.

### Apparatus and Procedure

The experimental apparatus used in the present study is similar to that employed by Tsai (Ref. 17). In brief, the split anode consisted of two identical copper dees of 76-mm (3-in.) diameter with their plane edges separated by an air gap of 0.1 mm (0.004 in.). This air gap serves as a thermal and electric insulator between the two copper dees. Both copper dees were water-cooled during experiments, as illustrated in Fig. 1.

The cathode was a 2% thoriated tungsten welding electrode of 2.4- or 3.2-mm (3/32- or 1/8-in.) diameters. The electrode was machined to an included angle of 50

or 75 deg with a 0.5-mm (0.02-in.) diameter truncation at the tip. A programmable gas tungsten arc (GTA) welding machine was used as the power source. Direct current, electrode negative (straight polarity) GTA welding was operated with a 0.567-$m^3$/hr (20-cfh) argon shielding gas.

The temperature rises of the cooling water passing through the copper dees were sensed by means of differential thermistors (Omega 44201), as shown in Fig. 1. The water flow rates were measured using turbine flowmeters and were maintained within ±0.005 gpm (0.019 L/min). The electric pulse signals generated by the flowmeters were amplified and converted to analog values. At the upstream of the water line, a water deoxygenator was used to remove dissolved oxygen in the water so that gas nucleation would not occur as the water temperature increased.

For the measurement of the current-density distribution, electric current was measured across a shunt of 0.0005-ohm resistance placed in the circuit. A PDP-11/73 data acquisition system with an analog-digital converter was used to record the data.

The split anode was mounted flat on a horizontally travelling stage driven by a synchronous motor at a speed of 1.8 mm/min (0.07 ipm). The arc was initially positioned on one copper dee, and the horizontal stage was driven so that the splitting plane of the anode moved across the arc in the direction perpendicular to itself.

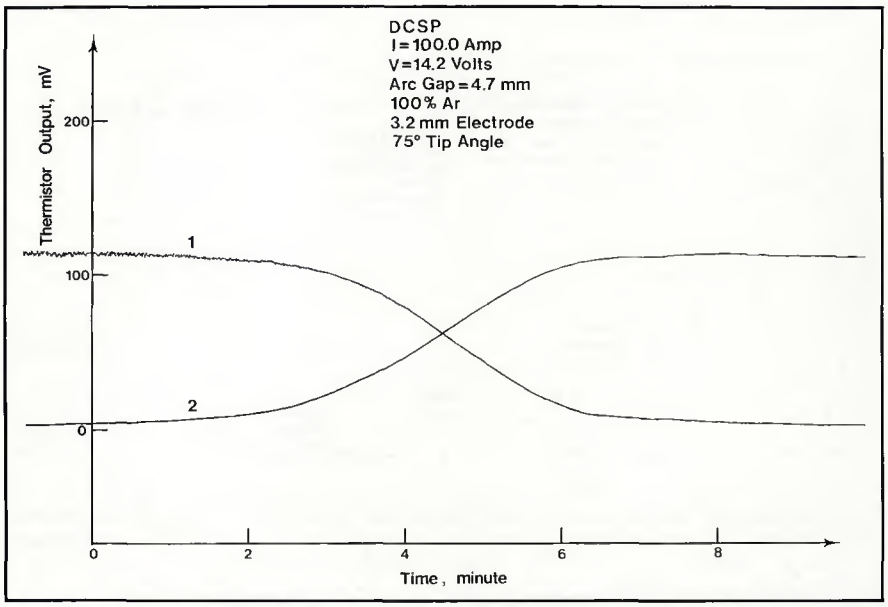


*Fig. 3 — Thermistor outputs, due to temperature rises in cooling water passing through copper dees, recorded as a function of time*

#### Data Analysis

An example of thermistor outputs as a function of time is shown in Fig. 3. Curve 1 shows the result from the cooling water passing through the copper dee upon which the arc was initiated, while Curve 2 shows that from the other copper dee. The heat transfer rate F(x) as a function of the arc position x can be obtained from the results shown in Fig. 3, using the travel speed of the anode and the following equation:

$$F(x) = \Delta T(x)\, C\rho W(x)$$

where $\Delta T(x)$ is the temperature rise determined from the output from the differential thermistors. C, $\rho$ and W(x) are, respectively, the specific heat, density and flow rate of the cooling water. The results obtained were treated with spline smoothing (Ref. 18).

The following methods were used to derive the radial distribution of the power density f(r) from the smoothed data of F(x):

1) Derivation of the distribution function from Nestor's tabulated values (Ref. 13).

2) Numerical integration using Equation 3, with the values of the double derivative F″(x) taken from the smoothed data.

3) Approximation of the recorded data F(x) with a high polynomial function and integration using Equation 3 with F″(x) derived from the polynomial function (Ref. 17).

4) Dividing the circular area of radius R into N annuli and solving the resultant N linear simultaneous equations for the distribution function by backward substitution (Ref. 15).

5) Using a statistical approach called "non-parametric minimization" and constraints set forth by the characteristics of the power-density distribution. Exponential functions were also tried in Method 3.

The first three methods were used by Tsai (Ref. 17). They were also used in the early stage of the present study. Because the double derivative of the measured F(x) is very sensitive to experimental noises, Methods 1 and 2 resulted in unstable and abnormal values. An approximation with a high order polynomial function produced results similar to Methods 1 and 2. An approximation with an exponential function resulted in a monotonically decreasing radial distribution, but oftentimes, the value at the origin of the distribution curve was not physically meaningful. In fact, in Abel transformation, all of the above three methods involve either a single or double derivative of measured F(x), and as a result, the distribution function obtained tends to be unstable and abnormal.

Since Method 4 involves no derivatives of F(x), it generally yielded results better than those produced by the above three methods. The circular area of radius R was divided into N annuli, and the resultant N-linear simultaneous equations were solved for the distribution function by backward substitution. The detailed calculation procedure has been described by Schoeck (Ref. 15). Due to the experimental error in F(x) and the statistical error propagation in the backward substitution, the resultant distribution function f(r) was not always monotonically decreasing from the center to the edge of the arc. This problem is illustrated in Fig. 4, using the results from Fig. 3. As shown, according to this method (Method 4), the power density of the arc, while decreasing from the center to the edge of the arc, increases suddenly at the radii of about 2.8, 5.2 and 6.5 mm (0.1, 0.2 and 0.25 in.).

In order to overcome the above-mentioned problem, a new method was developed in the present study. This method utilizes a statistical approach called non-parametric minimization and incorporates constraints set forth by the characteristics of the power-density distribution. Specifically, the distribution function f(r) is sought by minimizing the statistical difference between the experimentally measured data of F(x) and the corresponding values projected from the function, *i.e.*, $2\int_x^R f(r)\, r \cos^{-1}(x/r)\, dr$, without specifying the form (in terms of parameters) of the function first, and with the following two constraints being considered. First, the power density of the arc should be maximum at the center of the arc and decrease toward the edge. Second, the power-density distribution, when integrated over the area under the arc, should yield a power equal to the actual power delivered from the arc. The

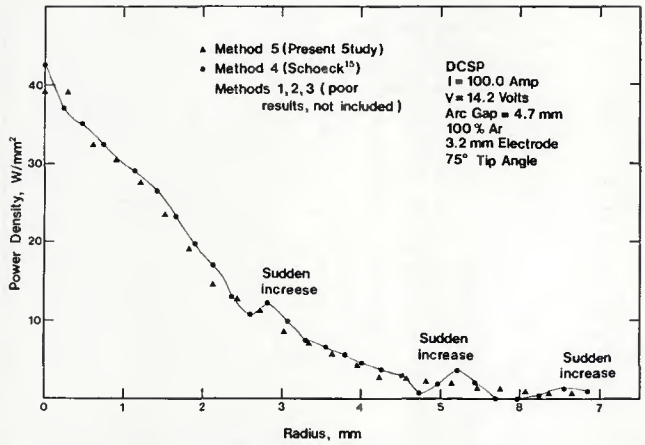


*Fig. 4—Comparison between power-density distributions, determined from two different methods of data analysis*

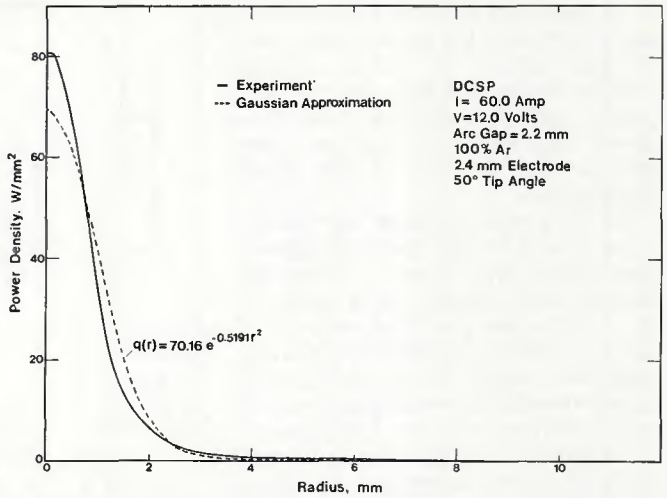


*Fig. 5—Power-density distribution in a 60-A arc with a 2.2-mm arc length. The electrode diameter is 2.4 mm*

formulation of this method is given as follows.

Equation 1, which gives the relationship between the measured function F(x) and the desired function f(r), is expressed in the following summation form. For any $x_k$,

$$F(x_k) = 2 \sum_{i=k}^{N} f_i r_i \cos^{-1}(x_k/r_i)\,\Delta r$$

$$= \sum_{i=k}^{N} f_i A_{k,i}$$

where $f_i = f(r_i)$.

The residual, which is defined as the difference between the observed and fitted values, is

$$F(x_k) - \sum_{i=k}^{N} f_i A_{k,i}$$

The residual sum of squares (SS), which is called the objective function and is a function of $f_1, f_2, \ldots f_N$, can be written as

$$SS(\vec{f}) = \sum_{k=1}^{N} \left(F(x_k) - \sum_{i=k}^{N} f_i A_{k,i}\right)^2$$

where

$$\vec{f} = \begin{pmatrix} f_1 \\ \cdot \\ \cdot \\ \cdot \\ f_N \end{pmatrix}$$

The two constraints mentioned previously can be expressed as follows.

1) $f_1 = f_2 > f_3 > \ldots > f_N \geq 0$

2) $2 \sum_{i=1}^{N} f_i A_{1,i} = Q$

where Q is the power delivered from the arc to the anode. Since the power density is at its maximum at the center of the arc, the slope of the power-density distribution curve should be zero there, and this is approximated by setting $f_1 = f_2$.

Similarly, for determining the current-density distribution, the objective function can be written as

$$SS(\vec{j}) = \sum_{k=1}^{M} \left(J(x_k) - \sum_{i=k}^{M} j_i A_{k,i}\right)^2$$

where j is the current-density vector, and $J(x_k)$ is the measured current. The two constraints are

1) $j_1 = j_2 > j_3 > \ldots > j_M \geq 0$

2) $2 \sum_{i=1}^{M} j_i A_{1,i} = I$

where I is the welding current.

A statistical procedure called "extended gradient projection" (Ref. 19) was used to carry out the minimization under the two constraints. The results are shown in Fig. 4. As shown, the power density decreases monotonically from the center to the edge of the arc.

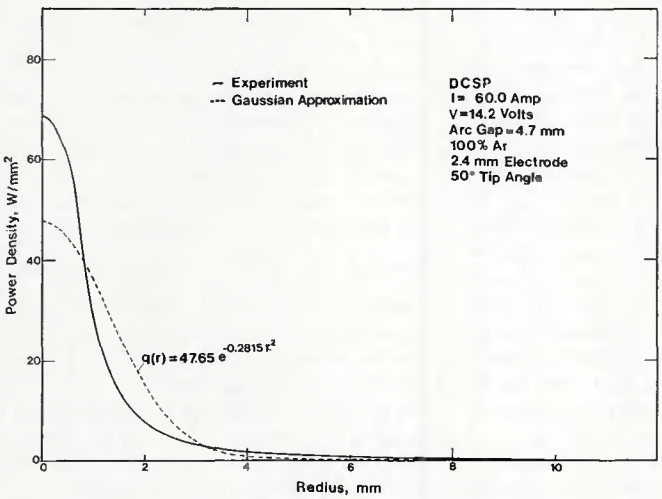


*Fig. 6—Power-density distribution in a 60-A arc with a 4.7-mm arc length. The electrode diameter is 2.4 mm*

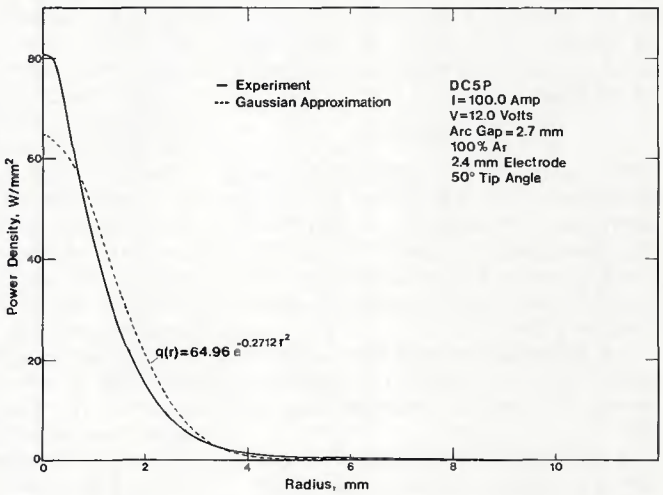


*Fig. 7—Power-density distribution in a 100-A arc with a 2.7-mm arc length. The electrode diameter is 2.4 mm*

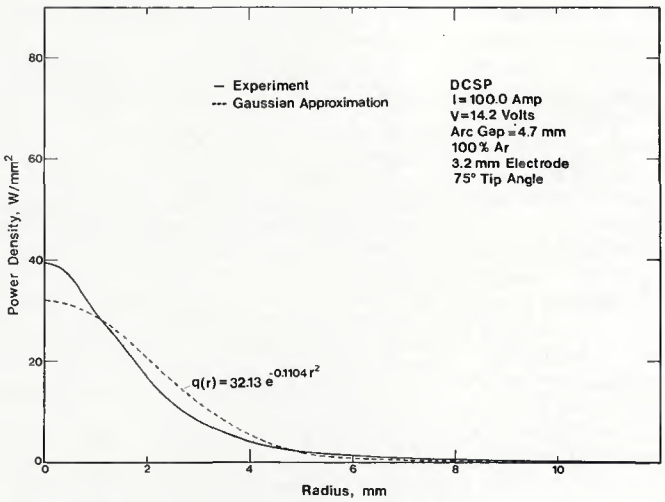


*Fig. 8 — Power-density distribution in a 100-A arc with a 4.7-mm arc length. The electrode diameter is 3.2 mm*

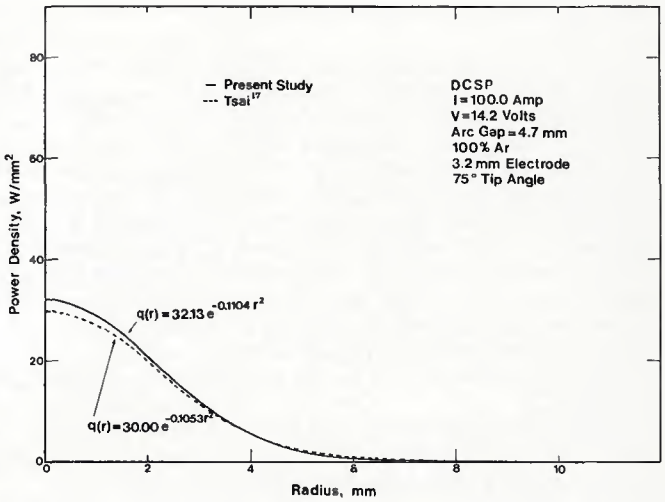


*Fig. 9 — Comparison between power-density distributions in the present and a previous study*

## Results and Discussion

Figure 5 shows the result of the power-density distribution in a gas tungsten arc of direct current and electrode negativity (DCEN). The welding current and the arc voltage were 60 A and 12 V, respectively. The shielding gas was pure argon, and the arc length was 2.2 mm (0.09 in.). The electrode had a 2.4-mm (3/32-in.) diameter and a 50-deg tip angle. As shown, the power density has a maximum value of about 80 W/mm$^2$ at the center of the arc and drops to essentially zero at a radius of about 3 mm (0.12 in.).

The experimental result shown in Fig. 5 was approximated with a Gaussian distribution of the form $q(r) = A \exp(-cr^2)$. The two parameters A and c were determined by meeting the following two conditions: 1) the integration of q (r) over the anode area equals the power delivered from the arc Q; and 2) the area under the Gaussian distribution curve equals that under the experimental distribution curve (Ref. 17). As shown in Fig. 5, the experimental distribution curve is steeper than the Gaussian one. However, the Gaussian distribution curve appears to be a reasonable approximation in this case.

Figure 6 shows the result of the power-density distribution in a gas tungsten arc under a welding condition identical to that shown in Fig. 5, except that the arc voltage (14.2 V) and the arc length (4.7 mm/0.19 in.) were higher. As expected, the maximum power density at the center of the arc is lower than that shown in Fig. 5, while the power density near the outer regions — at the radius of 3 mm, for example — is higher. This effect of arc length is consistent with that reported in previous studies (Refs. 13, 17).

The result shown in Fig. 6 reveals the interesting and important point that the Gaussian distribution is in fact a poor approximation in this case.

Figure 7 shows the result of the power-density distribution in a gas tungsten arc under a welding condition similar to that shown in Fig. 5, but with a higher welding current of 100 A. As shown, the power density is generally higher than that in Fig. 5. However, little difference exists between the two in the region near the center of the arc. This is perhaps due to the fact that the arc length (2.7 mm/0.11 in.) is somewhat greater in this case and that the maximum power density is already rather high and is, therefore, difficult to further increase.

An experiment was also carried out using a larger electrode of 3.2-mm (1/8-in.) diameter with a 75-deg tip angle. The welding current and arc length were 100 A and 4.7 mm, respectively. The result of the power-density distribution is shown in Fig. 8. As shown, the maximum power density is much lower than those shown in Figs. 5 to 7, thus indicating that the steepness in the power-density distribution is significantly reduced by increasing the electrode diameter.

Welding conditions close to that in Fig. 8 have been used by Tsai (Ref. 17), and it is, therefore, desirable to compare the results in the present study with those in Tsai's study. Unfortunately, all results in Tsai's work were presented in the form of Gaussian's distribution, and no original experimental distribution curves or data were available for direct comparison. Because of this, it was necessary to compare the Gaussian approximation to the experimental distribution curve in Fig. 8 against a corresponding Gaussian distribution from Tsai's work. The agreement, as shown in Fig. 9, appears to be reasonably good, even though the comparison was indirect.

The measured current-density distribution for the gas tungsten arc shown in Fig. 7 is shown in Fig. 10. As shown, the current-density distribution covers a narrower area on the anode surface than the corresponding power-density distribution shown in Fig. 7, thus suggesting that only the inner core of the arc plasma is sufficiently ionized to be electrically conductive. This is consistent with previ-

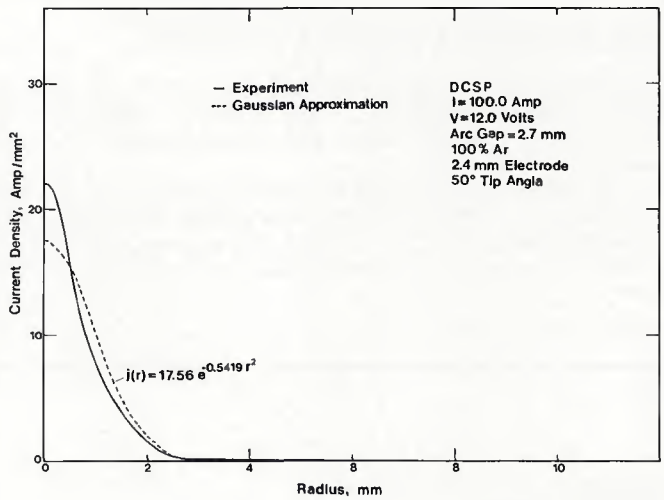


*Fig. 10 — Current-density distribution in a 100-A arc with a 2.7-mm arc length. The electrode diameter is 2.4 mm*

ous reports on arc measurements (Refs. 13, 17).

Finally, it must be pointed out that the power- and current-density distributions measured using the split-anode technique may differ from those in actual arc welding for the following reasons.

1) In actual arc welding, the metal under the arc is the liquid metal in the weld pool, rather than a piece of water-cooled copper. Therefore, the anode surface may not be flat due to the depression of the weld pool surface, which has been reported to occur under high welding currents, say, greater than about 225 A.

2) Evaporation of liquid metal in the weld pool may possibly result in some changes in the electrical conductivity of the arc plasma.

3) When welding at high speeds and arc lengths, the outer regions of the arc plasma may become somewhat elongated in the direction opposite to that of welding. However, since the present study was carried out in conjunction with research on the gas tungsten arc welding of aluminum sheets, where welding currents and speeds are both relatively small, the problems mentioned above are not expected to be significant.

## Conclusions

1) A new method has been developed for determining the power- and current-density distributions in welding arcs from experimental data generated by the split-anode technique. The method is based on a statistical approach called non-parametric minimization.

2) The new method is superior to previous methods due to the fact that it is stable, and constraints set forth by the characteristics of the power- and current-density distributions in a welding arc can be incorporated, so that the distributions obtained are physically meaningful.

3) The power- and current-density distributions in gas tungsten arcs are in general steeper than those based on the Gaussian distribution, and the Gaussian distribution can in some cases be a poor approximation.

4) The effects of the arc length, electrode diameter and welding current on the power- and current-density distributions observed in the present study are consistent with those reported previously.

*Acknowledgments*

The authors gratefully acknowledge support for this study from the National Science Foundation, under NSF Grant No. DMR 8419274. They would like to thank Professor C. F. Wu of the Department of Statistics, University of Wisconsin, for his help in the statistical analysis of the experimental data.

*References*

1. Rosenthal, D. 1941. *Welding Journal* 20(4):220–234.
2. Savage, W. F., Strunk, S. S., and Ishikawa, Y. 1965. *Welding Journal* 44(11):489-s to 496-s.
3. Key, J. F. 1980. *Welding Journal* 59(12): 365-s to 370-s.
4. Kou, S., and Le, Y. 1983. *Metallurgical Transactions A* 14A:2245.
5. Oreper, G. M., Eagar, T. W., and Szekely, J. 1983. *Welding Journal* 62(11):307-s to 312-s.
6. Oreper, G. M., and Szekely, J. 1984. *Journal of Fluid Mechanics* 147:53.
7. Szekely, J., Oreper, G. M., and McKelliget, J. 1986. *Modeling and Control of Casting and Welding Processes.* Edited by S. Kou and R. Mehrabian, The Metallurgical Society, p. 247.
8. Kou, S., and Sun, D. K. 1985. *Metallurgical Transactions A* 16A:203.
9. Kou, S., and Wang, Y. H. 1986. *Welding Journal* 65(3):63-s to 70-s.
10. Kou, S., and Wang, Y. H. 1986. *Metallurgical Transactions A* 17A:2271.
11. Wang, Y. H., and Kou, S. 1986. *Modeling and Control of Casting and Welding Processes.* The Metallurgical Society, p. 197.
12. Wang, Y. H., and Kou, S. 1986. *Advances in Welding Science and Technology.* Edited by S. A. David, ASM International, Metals Park, Ohio, p. 65.
13. Nestor, O. H. December 1959. Ph.D. Thesis, University of Buffalo, N. Y.
14. Nestor, O. H. 1967. *Journal of Applied Physics* 33:1638.
15. Schoeck, P. A. October 1961. Ph.D. Thesis, University of Minnesota, Minneapolis, Minn.
16. Schoeck, P. A. 1963. *Modern Developments in Heat Transfer.* Academic Press, New York, N.Y., p. 353.
17. Tsai, N. 1983. Ph.D. Thesis, Massachusetts Institute of Technology, Cambridge, Mass.
18. *Spline Smoothing Routines.* January 1979. Academic Computing Center, University of Wisconsin, Madison, Wis.
19. *Extended Gradient Projection Method.* January 1983. Academic Computing Center, University of Wisconsin, Madison, Wis.

Revised WRC Bulletin 297
September 1987

**Local Stresses in Cylindrical Shells Due to External Loadings on Nozzles—Supplement to WRC Bulletin 107 (Revision I)**

**By J. L. Mershon, K. Mokhtarian, G. V. Ranjan and E. C. Rodabaugh**

This Revised Bulletin 297 is intended as a replacement for the current supplement to Bulletin 107 and is specifically applied to cylindrical nozzles in cylindrical vessels. It replaces WRC Bulletin 297, August 1984. The changes in the text, figures and tables to update the 1984 edition of Bulletin 297 are described in the "Foreword to Revision I."

This revised Bulletin was prepared by the Subcommittee on Reinforced Openings and External Loadings of the Pressure Vessel Research Committee of the Welding Research Council. The price of Revised Bulletin 297, September 1987, is $24.00 per copy, plus $5.00 for postage and handling. Orders should be sent with payment to the Welding Research Council, Suite 1301, 345 E. 47th St., New York, NY 10017.